Inorganic Chemistry

Article

pubs.acs.org/IC

Anion-Exchange and Anthracene-Encapsulation within Copper(II) and Manganese(II)-Triazole Metal–Organic Confined Space in a Single Crystal-to-Single Crystal Transformation Fashion

Ju-Yan Liu, Qian Wang, Li-Jun Zhang, Bin Yuan, Yao-Yao Xu, Xin Zhang, Cong-Ying Zhao, Dan Wang, Yue Yuan, Ying Wang,* Bin Ding,* Xiao-Jun Zhao,* and Min Min Yue

Tianjin Key Laboratory of Structure and Performance for Functional Molecules; Key Laboratory of Inorganic–Organic Hybrid Functional Material Chemistry, Ministry of Education; College of Chemistry, Tianjin Normal University, Tianjin 300387, China

Supporting Information

ABSTRACT: A new multidentate ligand 1-(9-(1*H*-1,2,4-triazol-1-yl)anthracen-10-yl)-1*H*-1,2,4-triazole (tatrz) was designed and synthesized. Using tatrz as a building block, three novel coordination frameworks, namely, $\{[Cu(tatrz)_2(NO_3)_2]\cdot(CH_3OH)\cdot 4H_2O\}_n$ (**1**), $\{[Cu(tatrz)_2(H_2O)_2](BF_4)_2\}_n$ (**2**), and $[Mn(tatrz)_2(SCN)_2(CH_3OH)]\cdot 2H_2O$ (**3**) can be isolated. Anion-exchange experiment indicates that NO_3^- anions in the two-dimensional (2D) copper framework of **1** can be completely exchanged by ClO_4^- in an irreversible single crystal-to-single crystal (SC-SC) transformation fashion, as evidenced by the anion-exchange products of $\{[Cu(tatrz)_2(H_2O)_2](ClO_4)_2\cdot 4CH_3OH\}$ (**1a**). Further, if **1a** was employed as a precursor in *N*,*N*-dimethylformamide (DMF), an isomorphic solvate of $\{[Cu(tatrz)_2(DMF)_2](ClO_4)_2\cdot 2H_2O\}_n$ (**1b**) can be generated during the reversible dynamic transformation process. When **1** was immersed in CH_3OH, a distinct 2D layer $\{[Cu(tatrz)_2(NO_3)_2]\cdot 4.4CH_3OH\cdot 0.6H_2O\}_n$ (**1c**) was isolated. Interestingly, the solvent-exchange conversion is also invertible between **1** and **1c**, which exhibits spongelike dynamic behavior with retention of crystalline integrity. If the 2-fold interpenetrating three-dimensional (3D) framework **2** is selected, it can be transformed into another 2-fold interpenetrating 3D framework $\{[Cu(tatrz)_2(H_2O)_2](ClO_4)_2\cdot 5.56H_2O\}_n$ (**2a**) in a reversible SC-SC transformation fashion. However, when the light yellow crystals of mononuclear complex **3** were exposed to trichloromethane containing aromatic organic anthracene (atan), through our careful observation, the crystals of **3** were dissolved and reassembled into dark brown crystals of 2D crystalline coordination framework $\{[Mn(tatrz)_2(SCN)_2]\cdot(atan)\}_n$ (**3a**). X-ray diffraction revealed that in **3a**, atan acting as an organic template was encapsulated in the confined space of the 2D grid. Luminescent measurements illustrate that **3a** is the first report of multidimensional polymers based on triazole derivatives as luminescent probes of Mg^{2+}.

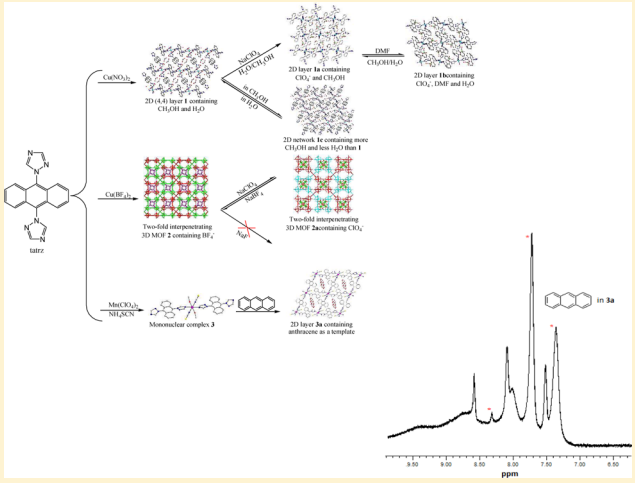

INTRODUCTION

In recent years a new class of microporous molecular-based materials known as porous coordination polymers (PCPs) or porous metal–organic frameworks (PMOFs) has received more and more not only fundamental but also industrial attention.[1−3] Their encapsulation inside the PMOF hydrophobic cavity is mainly based on optimal filling of the cavity volume, rather than on specific interactions. It is believed that nature abhors a vacuum and interpenetration reduces voids; therefore, large internal surface area and enhanced porosity are in contrast to the presence of interpenetrating lattices.[4] These coordination polymers consist of different metal atoms or metal clusters (secondary building units (SBUs)) and versatile rigid multidentate organic ligands (linkers).[1] However, these molecular-based containers, also defined as flasks or capsules, have many intriguing features: (i) they present confined chemical/physical environments, which can act as research platforms for molecular recognition, guest–host chemistry, catalysis, and molecule/ion sensing; (ii) they can be easily assembled in one step by combining relatively simple components through reversible supramolecular interactions; and (iii) they are often aesthetically appealing. These frameworks can reach high pore volumes and large surface areas.[4−7] Because of the high porosity, tunable pore size, and tunable functionality, PMOFs are predestinated for wide applications in many research areas such as gas storage,[8−12] separation,[13−15] catalysis,[16−18] and drug delivery.[19,20]

Received: January 24, 2014
Published: May 27, 2014

   dx.doi.org/10.1021/ic500183b | *Inorg. Chem.* 2014, 53, 5972−5985

Nowadays PMOFs with a dynamic behavior have received considerable interest because these functional coordination frameworks can exhibit a guest-induced structural change of the host lattice.[21] These porous frameworks contain potential or strain energy and undergo dramatic changes in functional properties and structure with the release of energy in response to specific external stimuli.[22,23] An appropriate external stimulus can perturb the coordination sites of porous frameworks and its connectivity by inducing the breaking and generating of coordination bonds.[24−26] Such a specific research system can offer researchers an experimentally unexplored field to investigate and expand the subtle intermediate region between flexibility and robustness through a dynamic single crystal-to-single crystal (SC-SC) and/or solid transformation process, involving cooperative movements of atoms in the solid state, which has attracted considerable attentions in recent years.[27] The SC-SC transformation is extremely desirable and useful, although it occurs relatively rarely, because it allows unequivocal assignment of the obtained product.[28] So far, most of the reports regarding SC-SC transformation described the breathing of three-dimensional (3D) porous materials through solvent exchange.[29] Recent research in our group is mainly focused on the study of anion recognition and anion separation with self-assembled receptors.[30] Along this line, the interest of developing novel metal-based anion receptors that can function efficiently and selectively in aqueous or organic-solvent environments has been particularly put first by many chemical researchers. This is a challenging target; a number of anions have high free hydration energies, and, thus, are not easy to bind and extract from water.[31−34]

Generally, the preparation of such materials can be influenced by a number of factors, such as crystallization conditions, ligand/metal ratio, reaction systems of different solvents, the nature of organic linkers, and so on. Particularly, the organic building blocks play an important role in the construction of PMOFs with versatile structures. It is widely known that the five-membered heterocycles, such as imidazole, pyrazole, triazole, and tetrazole, are good candidates in the design and synthesis of functional MOFs. Among them, 1,2,4-triazole and its derivatives have attained great interest as multidentate ligands, which can bridge different metal centers to construct many novel coordination functional frameworks because of their versatile bridging fashions.[35] As illustrated in the previous literatures, these reported triazole-containing ligands can be divided into two types: one contains flexible alkyl spacers, while the other contains rigid phenyl spacers.[36] However, these triazole ligands directly binding anthracene (atan) spacers have never been investigated. In comparison with alkyl and benzene rings, atan is a good fluorophore, and its derivatives have been extensively used as the fluorescence sensors.[37,38] Some of their derivatives emit in the green region and were used as molecular probes in chemiluminescent formulations. On the basis of the above considerations, in this work, we designed and synthesized the new functional ligand 1-(9-(1*H*-1,2,4-triazol-1-yl)anthracen-10-yl)-1*H*-1,2,4-triazole (tatrz) (Chart 1). To the best of our knowledge, such L^2-symmetry semirigid anthracene-based ligand tatrz has never been reported in the coordination chemistry up to now. The development of new ligand systems continuously undertakes an important effect for the development of MOFs chemistry. With the help of different copper(II) and manganese(II) salts, tatrz building blocks were employed to construct a two-dimensional (2D) network $\{[Cu(tatrz)_2(NO_3)_2]\cdot(CH_3OH)\cdot 4H_2O\}_n$ (**1**), a 2-fold 3D framework $\{[Cu(tatrz)_2(H_2O)_2](BF_4)_2\}_n$ (**2**), and a discrete mononuclear $[Mn(tatrz)_2(SCN)_2(CH_3OH)]\cdot 2H_2O$ (**3**) network. Anion- and solvent-exchange experiments for **1** and **2** were determined in an SC-SC transformation fashion. On the other hand, interestingly, when the light yellow crystals of **3** were exposed to atan in trichloromethane, the crystals of **3** dissolved and reassembled into dark brown crystals of 2D crystalline framework $\{[Mn(tatrz)_2(SCN)_2]\cdot(atan)\}_n$ (**3a**), which encapsulated atan as a template after slow evaporation for about 3 weeks. Such transformation process also represents the first example of metal−triazole coordination polymers containing atan and an exceedingly rare example of reassembly from a zero-dimensional (0D) complex to a 2D sheet. Luminescent measurements indicate that **3a** is the first report of multidimensional polymers based on triazole drivatives as luminescent probes of Mg^{2+}.

Chart 1. A Schematic Presentation of Tatrz

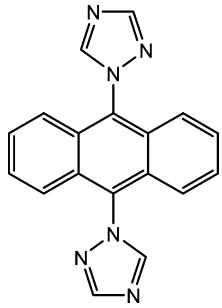

EXPERIMENTAL SECTION

General Remarks. All the reagents are commercially available and used without further purification. The elemental analysis of carbon, nitrogen, and hydrogen was measured on a PerkinElmer 240 elemental anaoyzer. Powder X-ray diffraction analysis was determined on a D/Max-2500 X-ray diffractometer using Cu Kα radiation. ^{1}H NMR data were measured using a Bruker Avance 400 MHz spectrometer. Chemical shifts are reported in δ relative to tetramethylsilane. The photoluminescence spectra were recorded by a MPF-4 fluorescence spectrophotometer with a xenon arc lamp as the light source. The 2−300 K variable-temperature magnetic susceptibilities were measured on a Quantum Design MPMS-7 SQUID magnetometer. The 1000 Oe magnetic field was applied in the magnetic measurement. For all the constituent atoms, diamagnetic corrections were applied with Pascal's constants.

Synthesis of 1-(9-(1*H*-1,2,4-Triazol-1-yl)anthracen-10-yl)-1*H*-1,2,4-triazole (tatrz). 9,10-Dibromoanthracene was synthesized by procedures reported earlier.[39] Then 9,10-dibromoanthracene (0.92 g, 2.74 mmol), 1*H*-1,2,4-triazole (0.38 g, 5.48 mmol), K_2CO_3 (0.76 g, 5.48 mmol), and CuO (0.01 g, 0.125 mmol) were mixed and heated while stirring in 15 mL of dimethyl sulfoxide (DMSO) at the temperature of 150 °C for 2 d. The resulting suspending liquid was cooled to 25 °C, and solids were removed by filtration. Further the filtrate can be removed under vacuum distillation. The remaining filtrate was added by organic solvent of CH_2Cl_2; the resulting mixture was washed with deionized water and stored under vacuum overnight. Then organic solvent of CH_2Cl_2 was removed. The products were crystallized in methanol and deionized water, and deep yellow solids were obtained.

Synthesis of $\{[Cu(tatrz)_2(NO_3)_2]\cdot(CH_3OH)\cdot 4H_2O\}_n$ (1). A mixture of $Cu(NO_3)_2\cdot 3H_2O$ (0.0483 g, 0.2 mmol) and tatrz (0.0625 g, 0.2 mmol) was stirred for 0.5 h in deionized water (1 mL), trichloromethane (1 mL), and methanol (8 mL). The filtrate was evaporated at 25 °C for about half a month, and well-shaped green crystals suitable for X-ray diffraction analysis were isolated. Yield: 69%. Elemental

dx.doi.org/10.1021/ic500183b | Inorg. Chem. 2014, 53, 5972−5985

Table 1. Crystallographic Data and Details of Refinements for Complexes 1−3, 1a−3a, 1b, and 1c

	1	2	3	1a	2a	3a	1b	1c
formula	$C_{37}H_{38}CuN_{14}O_{12}$	$C_{36}H_{28}B_2CuF_8N_{12}O_2$	$C_{40}H_{34}MnN_{14}O_4S_2$	$C_{40}H_{44}Cl_2CuN_{12}O_{14}$	$C_{36}H_{41.13}Cl_2CuN_{12}O_{15.56}$	$C_{49}H_{33}MnN_{10}S_2$	$C_{42}H_{42}Cl_2CuN_{14}O_{12}$	$C_{40}H_{43}CuN_{14}O_{11}$
M (g mol^{-1})	934.35	897.86	893.87	1051.31	1025.42	880.91	1069.34	959.42
crystal system	triclinic	tetragonal	monoclinic	monoclinic	tetragonal	triclinic	monoclinic	triclinic
space group	$P\bar{1}$	$I4(1)/a$	$P2(1)/n$	$P2(1)/c$	$I4(1)/a$	$P\bar{1}$	$P2(1)/c$	$P1$
temperature	113(2)	113(2)	173(2)	296(2)	113(2)	113(2)	113(2)	113(2) K
a (Å)	8.368(2)	14.3290(12)	7.1626(4)	10.6944(11)	14.353(2)	13.514(3)	10.009(3)	8.4650(17)
b (Å)	10.586(2)	14.3290(12)	27.2309(16)	13.9742(14)	14.353(2)	14.027(3)	13.956(4)	10.542(2)
c (Å)	13.162(3)	44.554(4)	11.2131(7)	15.8189(17)	44.533(9)	14.082(3)	16.491(5)	13.191(3)
α (deg)	67.860(7)	90	90	90	90	117.25(3)	90	68.17(3)
β (deg)	76.771(9)	90	98.5950(10)	107.169(2)	90	106.18(3)	105.060(4)	77.17(3)
γ (deg)	89.873(12)	90	90	90	90	100.13(3)	90	89.70(3)
V (Å^3)	1046.7(4)	9147.8(14)	2162.5(2)	2258.7(4)	9175(3)	2130.3(8)	2224.5(10)	1061.5(4)
Z	1	8	2	2	8	2	4	1
F(000)	483	3640	922	1086	4229	908	1102	498
ρ_{calc} (Mg m^{-3})	1.482	1.304	1.373	1.546	1.485	1.373	1.596	1.501
μ (mm^{-1})	0.601	0.554	0.460	0.683	0.673	0.457	0.693	0.593
data/restraints/params	4908/3/319	5457/56/313	3797/25/305	3990/88/329	4521/101/342	7359/0/563	5297/3/330	4798/9/341
GOF on F^2	1.083	1.084	1.062	1.039	1.125	1.197	1.039	1.103
$R_1{}^a$ ($I = 2\sigma(I)$)	0.0458	0.0564	0.0533	0.0600	0.0816	0.1756	0.0496	0.0543
$\omega R_2{}^b$ (all data)	0.1401	0.1428	0.1478	0.1766	0.2337	0.4956	0.1359	0.1521

$^aR_1 = \Sigma||F_0| - |F_c||/|F_0|$. $^b\omega R_2 = [\Sigma w(|F_0|^2 - |F_c^2|^2/w|F_0^2|^2]^{1/2}$.

dx.doi.org/10.1021/ic500183b | Inorg. Chem. 2014, 53, 5972−5985

Table 2. Selected Bond Lengths [Å] and Angles [deg] for 1−3, 1a−3a, 1b, and 1c

1[a]					
Cu(1)−N(4)	2.018(2)	Cu(1)−N(1)	2.032(2)	Cu(1)−O(1)	2.3983(19)
N(4)−Cu(1)−N(1)	88.37(8)	N(4)−Cu(1)−O(1)	83.38(8)	N(4A)−Cu(1)−N(1)	91.63(8)
N(1)−Cu(1)−N(1)#1	180.00(11)	N(1)−Cu(1)−O(1)	97.79(8)	N(4)#1−Cu(1)−N(4)	179.999(2)
N(4)#1−Cu(1)−N(1)	91.63(8)	N(4)−Cu(1)−O(1)#1	96.62(8)	N(1)−Cu(1)−O(1)#1	82.21(8)
2[a]					
Cu(1)−N(1)#1	2.0266(19)	Cu(1)−N(1)	2.0267(19)	Cu(1)−N(6)#2	2.0286(19)
Cu(1)−O(1)	2.3693(18)	N(1)−Cu(1)−N(6)#3	90.38(8)	N(1)#1−Cu(1)−N(1)	88.80(11)
O(1)−Cu(1)−O(1)#1	178.81(10)	N(6)#2−Cu(1)−N(6)#3	90.72(11)	N(1)#1−Cu(1)−O(1)	93.04(7)
N(1)−Cu(1)−O(1)	86.11(7)	N(1)−Cu(1)−N(6)#2	175.83(8)	N(6)#3−Cu(1)−O(1)	90.98(8)
N(6)#2−Cu(1)−O(1)	89.85(8)				
3[a]					
Mn(1)−N(7)	2.159(3)	Mn(1)−O(1)	2.207(2)	Mn(1)−N(3)	2.269(3)
N(7)#1−Mn(1)−N(7)	180.00(12)	N(7)#1−Mn(1)−O(1)#1	87.61(10)	N(7)−Mn(1)−O(1)#1	92.39(10)
N(7)−Mn(1)−O(1)	87.61(10)	O(1)#1−Mn(1)−O(1)	180.0	N(7)−Mn(1)−N(3)#1	91.68(10)
N(7)#1−Mn(1)−N(3)#1	88.33(10)	(1)#1−Mn(1)−N(3)#1	89.03(9)	O(1)−Mn(1)−N(3)#1	90.97(9)
1a[a]					
Cu(1)−O(5)	2.402(3)	Cu(1)−N(3)	2.034(3)	Cu(1)−N(6)#2	2.035(3)
N(3)#1−Cu(1)−N(3)	180.00(16)	N(3)−Cu(1)−N(6)#3	91.61(13)	N(3)#1−Cu(1)−O(5)	87.03(13)
N(3)−Cu(1)−O(5)	92.97(13)	N(6)#2−Cu(1)−O(5)	93.39(13)	N(6)#3−Cu(1)−O(5)	86.61(13)
N(6)#3−Cu(1)−O(5)	86.61(13)	O(5)−Cu(1)−O(5)#1	180.0	N(3)#1−Cu(1)−N(6)#2	88.39(13)
1b[a]					
Cu(1)−N(6)#1	2.0180(19)	Cu(1)−N(1)#3	2.0193(19)	Cu(1)−N(1)	2.0192(19)
Cu(1)−O(1)#3	2.3772(18)	Cu(1)−O(1)	2.3771(18)	O(1)−Cu(1)−O(1)#3	179.999(2)
N(6)#1−Cu(1)−N(6)#2	180.0	N(6)#1−Cu(1)−N(1)	87.27(8)	N(1)#3−Cu(1)−O(1)	87.18(7)
N(6)#1−Cu(1)−N(1)#3	92.73(8)	N(1)−Cu(1)−N(1)#3	180.0	N(6)#1−Cu(1)−O(1)	86.77(7)
N(1)#3−Cu(1)−O(1)#3	92.82(7)	N(6)#1−Cu(1)−O(1)#3	93.23(7)		
1c[a]					
Cu(1)−N(1)	2.020(2)	Cu(1)−N(4)	2.025(2)	Cu(1)−O(1)#1	2.388(2)
N(1)#1−Cu(1)−N(1)	180.0	(1)#1−Cu(1)−N(4)	91.87(10)	N(1)−Cu(1)−N(4)	88.13(10)
N(4)−Cu(1)−N(4)#1	180.00(13)	N(1)#1−Cu(1)−O(1)#1	96.95(9)	N(1)−Cu(1)−O(1)#1	83.05(9)
N(4)−Cu(1)−O(1)#1	96.18(9)	N(4)#1−Cu(1)−O(1)#1	83.82(9)	N(1)−Cu(1)−O(1)	96.95(9)
O(1)#1−Cu(1)−O(1)	179.999(1)				
2a[a]					
Cu(1)−N(4)#1	2.033(4)	Cu(1)−N(1)	2.036(4)	Cu(1)−O(1)	2.376(4)
N(4)#1−Cu(1)−N(4)#2	90.8(2)	N(4)#1−Cu(1)−N(1)#3	90.36(16)	N(4)#2−Cu(1)−N(1)#3	175.62(18)
N(4)#2−Cu(1)−N(1)	90.36(17)	N(1)#3−Cu(1)−N(1)	88.8(2)	N(4)#1−Cu(1)−O(1)	89.46(19)
N(4)#2−Cu(1)−O(1)	91.5(2)	N(1)#3−Cu(1)−O(1)	92.77(19)	N(1)−Cu(1)−O(1)	86.29(19)
O(1)−Cu(1)−O(1)#3	178.7(2)				
3a[a]					
Mn(1)−N(5)	2.181(10)	Mn(1)−N(3)	2.228(9)	Mn(1)−N(1)	2.323(10)
Mn(2)−N(10)	2.216(10)	Mn(2)−N(6)	2.236(9)	Mn(2)−N(8)	2.315(9)
N(5)#1−Mn(1)−N(5)	180.0	N(5)−Mn(1)−N(3)	89.2(4)	N(5)#1−Mn(1)−N(3)	90.8(4)
N(3)−Mn(1)−N(3)#1	179.999(4)	N(3)#1−Mn(1)−N(1)#1	85.8(4)	N(3)−Mn(1)−N(1)#1	94.2(4)
N(5)−Mn(1)−N(1)#1	89.6(4)	N(5)#1−Mn(1)−N(1)#1	90.4(4)	N(10)−Mn(2)−N(6)#2	88.9(4)
N(10)#2−Mn(2)−N(8)#2	88.8(3)	N(6)−Mn(2)−N(8)#2	93.4(3)	N(6)#2−Mn(2)−N(8)#2	86.6(3)
N(10)−Mn(2)−N(6)	91.1(4)	N(10)−Mn(2)−N(8)#2	91.2(3)		

[a]Symmetry transformations used to generate equivalent atoms: For **1**: #1 $-x+2, -y+1, -z+2$; For **2**: #1 $-x+1, -y+1/2, z+0$; #2 $y+1/4, -x+1/4, z+1/4$; #3 $-y+3/4, x+1/4, z+1/4$; For **3**: #1 $-x, -y, -z+1$; For **1a**: #1 $-x, -y+2, -z$; #2 $x-1, -y+3/2, z-1/2$; #3 $-x+1, y+1/2, -z+1/2$; For **2a**: #1 $-y+3/4, x-3/4, z+1/4$; #2 $y+1/4, -x+5/4, z+1/4$; #3 $-x+1, -y+1/2, z+0$; For **3a**: #1 $-x, -y+2, -z+1$; #2 $-x+1, -y+1, -z$; For **1b**: #1 $-x+1, y+1/2, -z+1/2$; #2 $x-1, -y+1/2, z-1/2$; #3 $-x, -y+1, -z$; For **1c**: #1 $-x+1, -y+1, -z+1$.

analysis calcd (%) for $C_{37}H_{38}CuN_{14}O_{12}$: C 47.56, H 4.10, N 20.99; found: C 47.68, H 4.08, N 20.88.

Synthesis of {[Cu(tatrz)$_2$(H$_2$O)$_2$](ClO$_4$)$_2$·4CH$_3$OH} (1a). A suspension mixture of **1** (0.4672 g, 0.5 mmol) and sodium perchlorate monohydrate (0.7023 g, 5 mmol) in water/methanol solutions (10 mL, v/v = 5:5) was stirred for 6 h. Well-shaped green block crystals suitable for X-ray diffraction analysis were isolated. Yield: 25%. Elemental analysis calcd (%) for $C_{40}H_{44}Cl_2CuN_{12}O_{14}$: C 45.70, H 4.22, N 15.99; found: C 45.58, H 4.02, N 15.78.

Synthesis of {[Cu(tatrz)$_2$(DMF)$_2$](ClO$_4$)$_2$·2H$_2$O}$_n$ (1b). A mixture of **1a** (0.5257 g, 0.5 mmol) in *N*,*N*-dimethylformamide (DMF) (10 mL) was stirred for 6 h. Well-shaped green block crystals suitable for X-ray diffraction analysis were isolated. Yield: 35%. Elemental analysis calcd (%) for $C_{42}H_{42}Cl_2CuN_{14}O_{12}$: C 47.17, H 3.96, N 18.34; found: C 47.26, H 4.08, N 18.28.

Synthesis of {[Cu(tatrz)$_2$(NO$_3$)$_2$]·0.6H$_2$O·4.4CH$_3$OH}$_n$ (1c). A mixture of **1** (0.4672 g, 0.5 mmol) in methanol solution (10 mL) was stirred for 6 h. Well-shaped green block crystals suitable for X-ray diffraction analysis were isolated. Yield: 42%. Elemental analysis calcd (%) for $C_{40}H_{43}CuN_{14}O_{11}$: C 50.08, H 4.52, N 20.44; found: C 50.26, H 4.48, N 20.58.

dx.doi.org/10.1021/ic500183b | Inorg. Chem. 2014, 53, 5972−5985

Synthesis of $\{[Cu(tatrz)_2(H_2O)_2](BF_4)_2\}_n$ (2). Complex **2** can be isolated as green rodlike crystals by a preparation procedure similar to that described for **1**, except with $Cu(BF_4)_2\cdot 6H_2O$ replacing $Cu(NO_3)_2\cdot 3H_2O$. Yield: 78%. Elemental analysis calcd (%) for $C_{36}H_{28}B_2CuF_8N_{12}O_2$: C 48.16, H 3.14, N 18.72; found: C 48.08, H 3.10, N 18.68.

Synthesis of $\{[Cu(tatrz)_2(H_2O)_2](ClO_4)_2\cdot 5.56H_2O\}_n$ (2a). A suspension mixture of **2** (0.4672 g, 0.5 mmol) and $NaClO_4\cdot H_2O$ (0.7023 g, 5 mmol) in water/methanol (10 mL, v/v = 1:1) was stirred for 6 h. Well-shaped green block crystals suitable for X-ray diffraction analysis were isolated. Yield: 25%. Elemental analysis calcd (%) for $C_{36}H_{41.13}Cl_2CuN_{12}O_{15.56}$: C 42.17, H 4.04 N 16.39; found: C 47.08, H 4.02, N 16.38.

Synthesis of $[Mn(tatrz)_2(SCN)_2(CH_3OH)]\cdot 2H_2O$ (3). Tatrz (0.3120 g, 1 mmol) and $Mn(ClO_4)_2\cdot 6H_2O$ (0.7240 g, 2 mmol) were dissolved in 15 mL of trichloromethane/methanol/water mixed solution (v/v/v = 3:10:2). The resulting mixture was stirred for 15 min, then the solid powder of ammonium thiocyanate (0.1520 g, 2 mmol) was added. The resulting brown-yellow solution was filtered off and left to stand at room temperature. Brownish-black crystals suitable for X-ray diffraction analysis were isolated within 1 week in a 45% yield. Elemental analysis calcd (%) for $C_{40}H_{34}MnN_{14}O_4S_2$: C 53.75, H 3.83, N 21.94; found: C 53.54, H, 3.88, N 21.89.

Synthesis of $\{[Mn(tatrz)_2(SCN)_2](atan)_2\}_n$ (3a). **3** (0.4469 g, 0.5 mmol) was immersed in atan in trichloromethane (10 mL). After stirring for 6 h, through our careful observations, all of the crystals of **3** were dissolved. The resulting mixture was evaporated in the dark at room temperature for about 3 weeks, and well-shaped brown-orange rodlike crystals suitable for single-crystal X-ray diffraction analysis were isolated. Yield: 35%. Elemental analysis calcd (%) for $C_{49}H_{33}MnN_{10}S_2$: C 66.80, H 3.78, N 15.90; found: C 66.95, H 3.89, N 16.02.

X-ray Crystallography. Single-crystal X-ray diffraction determination for compounds **1**−**3**, **1a**−**3a**, **1b**, and **1c** were collected on an APEX II CCD area detector and a Bruker Smart CCD diffractometer. A graphite crystal monochromator was equipped in the incident beam for data collection at the temperatures of 294(2) and 293(2) K, respectively. The $\omega-\varphi$ scan technique was applied. Direct methods were applied to solve the structures. Full-matrix least-squares methods using the SHELXL-97 and SHELXS-97 programs were used to refine the crystal structures.[40,41] For all the coordination complexes anisotropic thermal parameters were applied to all non-hydrogen atoms. Anomalous dispersion corrections were incorporated, and analytical expressions of neutral-atom scattering factors were also used. These crystallographic data and selected bond distances and bond angles of these title complexes are listed in Tables 1 and 2, respectively. Additional crystallographic information for this Paper is available in the Supporting Information.

RESULTS AND DISCUSSION

Structural Descriptions. Single-crystal X-ray diffraction analysis shows that coordination polymer **1** features a 2D layer framework and that the fundamental structure unit contains one Cu^{II} ion, two independent tatrz ligands, two terminal-coordinated nitrate anions, one CH_3OH, and four H_2O solvent molecules (Figure 1). Each central Cu^{II} ion lies in a crystallographic inversion center. The central Cu^{II} ion is also six-coordinated by two oxygen atoms of two axially nitrate anions and four $N_{triazole}$ atoms of four tatrz ligands in a square-planar fashion. The coordination sphere of six-coordinated Cu^{II} can be viewed as a slightly distorted octahedron. The Cu(1)−O(1) axial bond length (2.398(18) Å) is much longer in comparison with those previously reported Cu−O bond lengths (varying from 1.967(5) to 1.977(5) Å) in the triazole-Cu(II) coordination polymer $[Cu_3(\mu_3\text{-}OH)L_3(ClO_4)(H_2O)_2](ClO_4)\cdot 2H_2O$ (L = 3-acetylamino-1,2,4-triazolate),[42] which can be ascribed to Jahn−Teller elongation.

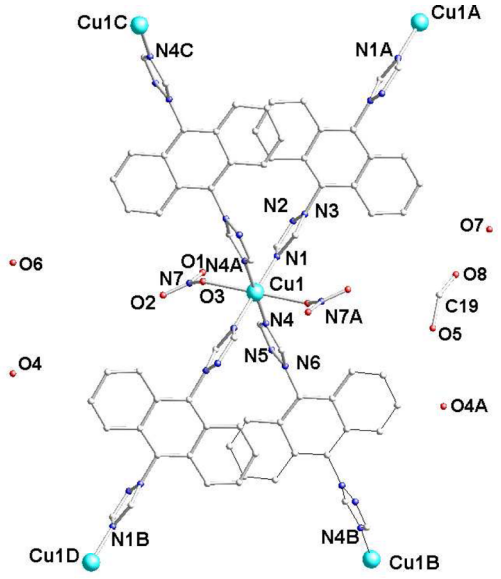

Figure 1. Fundamental structure unit of **1**. Gray, C; blue, N; red, O; cyan, Cu.

In **1**, each tatrz ligand serves as a μ_2-bridging ligand and connects two Cu^{II} ions by two $N_{triazole}$ atoms. Each central Cu^{II} ion is interlinked by four μ_2-tatrz bridging ligands, forming a rhombohedral grid with (4,4) topological network, as displayed in Figure 2a. All Cu^{II} ions in each layer are strictly coplanar, and

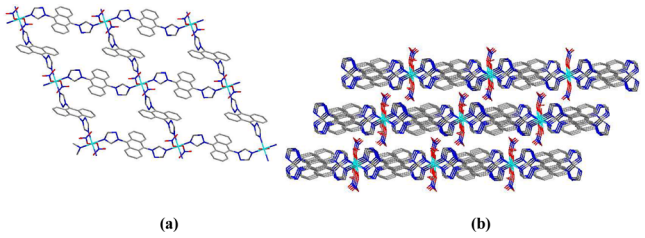

Figure 2. (a) 2D layer with (4,4) topology in **1**; (b) side view of **1** stacking in the ABCABC sequence, in which CH_3OH and H_2O molecules exist between the neighboring layers. Gray, C; blue, N; red, O; cyan, Cu.

nitrate anions exist up and down the 2D layer. The corresponding dihedral angles between atan rings and triazole moieties in tatrz in **1** are 70.3° and 88.8°, respectively, indicating strong spatial distortion effect. As depicted in Figure 2b, the neighboring 2D layers are densely stacked in an offset ABCABC··· stacking way, and the Cu···Cu separation along Cu···tatrz···Cu is 13.479(8) Å and 13.427(67) Å, respectively. Note that guest molecules (CH_3OH plus H_2O) are embedded in the adjacent 2D layers. To the best of our knowledge, such arrangement of 2D framework trapping CH_3OH molecules is still scarcely reported in the published literature. The free lattice water molecules and nitrogen and oxygen atoms from triazole ring and nitrate groups, respectively, are also involved in O−H···O and O−H···N hydrogen bonds (Figure 3a) with relatively linear coordination geometry (O−H···O and O−H···N angles being 176° and 175°, respectively). Such hydrogen bonds extend the 2D layer of **1** into the 3D supramolecular framework (Figure 3b).

When the same preparation method was employed with $Cu(BF_4)_2\cdot 6H_2O$ replacing $Cu(NO_3)_2\cdot 3H_2O$, complex **2** can be

dx.doi.org/10.1021/ic500183b | Inorg. Chem. 2014, 53, 5972−5985

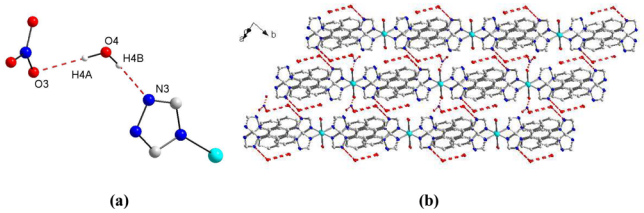

Figure 3. (a) The O−H···O and O−H···N hydrogen bonds between the lattice water molecule and trizaole ring or nitrate anion; (b) perspective diagram of the 3D hydrogen-bonding supramolecular framework of **1**. Gray, C; blue, N; red, O; white, H; cyan, Cu; red dotted line, hydrogen bond.

isolated. The asymmetric unit of **2** contains one cation $[Cu(H_2O)_2(tatrz)_2]^{2+}$ unit and two free BF_4^- anions (Figure 4). In this example, each octahedral Cu^{II} center also lies in the

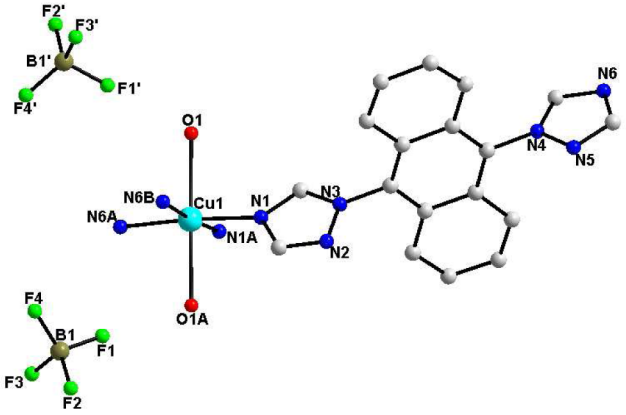

Figure 4. View of the Cu^{II} coordination environment in complex **2** with atom labeling of the asymmetric unit (hydrogen atoms are omitted for clarity). Gray, C; blue, N; red, O; cyan, Cu; green, F; brown, B.

inversion center. The central ion coordinates to two water molecules from an axial direction and four $N_{triazole}$ atoms of four tatrz ligands strictly in the coplanar. Each Cu^{II} center is coordinated by four tatrz ligands, while each tatrz tecton connects two neighboring Cu^{II} ions. The overall result ultimately constructs a 3D MOF framework, in which one-dimensional (1D) rhombic channels with the size of 10.102(23) × 14.067(33) $Å^2$ can be observed. The dihedral angles between the atan rings and triazole moieties of tatrz are 89.9° and 86.8°, respectively, indicating extremely strong spatial distortion effect. Topologically, if each Cu^{II} ion is considered as a basic node of a simplified network, then the central Cu^{II} ion can be viewed as four-connected nodes and each μ_2-tatrz tecton linkers, respectively. **2** can be defined as a 3D four-connected network with the Schläfli symbol of $6^5$8-$CdSO_4$ topology (Supporting Information, Figure S1). Significantly, PLATON[43] calculations based on the single-crystal X-ray structural parameters show that the void space volume are accommodated by the free BF_4^- anions approximately 3082.8 $Å^3$ (33.7% per unit cell volume). Because of the large cavity in the 3D framework of **2**, simultaneous 2-fold interpenetration of the network occurs along self-assembly, as displayed in Figure 5. Such mutual interpenetration of the network usually fills up potential cavities and reduces porosity. Interestingly, free BF_4^- anions and water molecules occupy the 1D square channels with the edge of 9.542 × 9.542 $Å^2$. Since the free rotated C_{atan}−

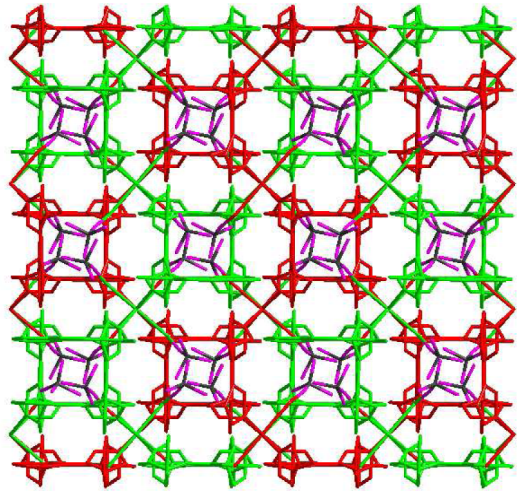

Figure 5. Perspective view of 2-fold interpenetrating structure of **2**. Brown, B; purple, F; red and green, two interpenetrating frameworks.

$N_{triazole}$ single bonds result in the flexibility of tatrz ligand, the triazole rings might be rotated by a certain angle, which makes the size of the 1D channel adjustable to fit anion exchange. It is also helpful to note that the coordinated aqua molecules (O1) and the fluorine atoms of BF_4^- anions participate in the formation of O−H···F hydrogen bonding (the bond angle of O−H···F is 170°). The O−H···O hydrogen bonding distances vary from 2.6123 to 2.6560 Å, which is much shorter than these previously reported O−H···O distances,[44] indicating strong hydrogen-bonding interactions. These weak intermolecular interactions play the key role in stabilizing the expanded 3D supramolecular framework (Supporting Information, Figure S2).

Note that adding NH_4SCN to the reaction system of tatrz and $Mn(ClO_4)_2·6H_2O$ gave single crystals of a mononuclear coordination complex $[Mn(tatrz)_2(SCN)_2(CH_3OH)]·2H_2O$ (**3**). As depicted in Figure 6, each Mn^{II} center is coordinated by two $N_{triazole}$ atoms from two tatrz ligands, two oxygen atoms from two CH_3OH molecules in the equatorial plane, and two nitrogen atoms from NCS^- anions at the axial positions completing the $[MnN_4O_2]$ octahedral coordination environment. The Mn−O(1) bond distance is 2.207(2) Å, whereas the Mn−N(3) and Mn−N(7) bond lengths are 2.269 (3) Å and 2.159 (3) Å, respectively. The Mn1, N(3), N(3A), N(7), and N(7A) atoms are almost coplanar (mean deviation from plane < 0.11 Å). The tatrz ligands coordinate to the central Mn^{II} ions through N(3) atom of triazole moiety, whereas N(6) atom of triazole moiety is uncoordinated. The dihedral angles between atan rings and triazole moieties of tatrz in **3** are 65.5° and 83.8°, respectively, while the dihedral angle between two triazole groups is 31.6°. Furthermore, O(2) atoms of free aqua molecules are involved in O−H···N hydrogen-bonding interactions with noncoordinating nitrogen atoms, further extending mononuclear complex **3** into a 3D supramolecular architecture (Supporting Information, Figure S3).

Powder X-ray Diffraction Studies and Thermal Stabilities. The powder X-ray diffraction (PXRD) patterns determined for the crystal materials of the title complexes and their calculated pattern deduced from single-crystal X-ray data are shown in Supporting Information, Figures S4−S11. They are in good agreement with PXRD patterns simulated from the corresponding single-crystal X-ray data, not only in respect of

dx.doi.org/10.1021/ic500183b | Inorg. Chem. 2014, 53, 5972−5985

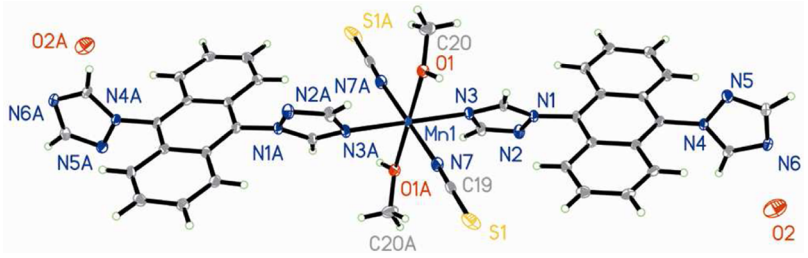

Figure 6. ORTEP diagram and atom labeling system for **3**.

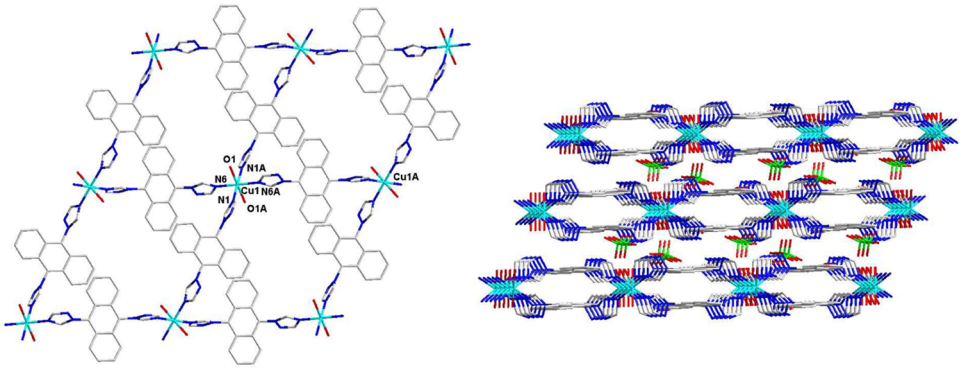

Figure 7. (a) 2D cation grid layer of **1a**; (b) side view of the 2D framework of **1a** stacking in the ABCABC··· way, in which free ClO_4^- anions exist between the neighboring 2D layers. Gray, C; blue, N; green, Cl; red, O; cyan, Cu.

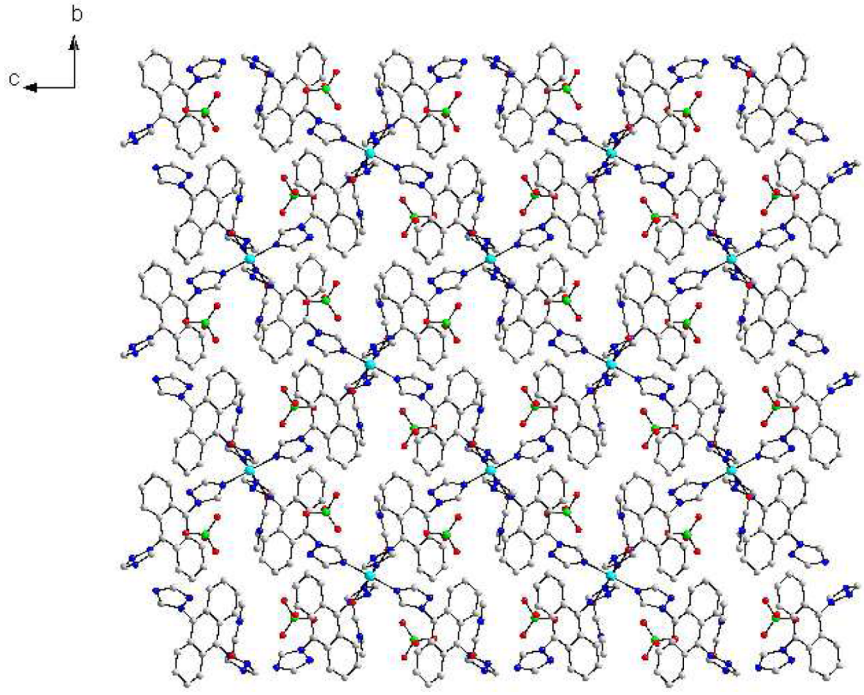

Figure 8. Perspective view of 2D layer along the *a* axis in **1a**. Green, Cl; red, O; gray, C; blue, N; cyan, Cu.

the sharpness of the lines but also the position of the peaks. The result also reveals that the single-crystal structures are representative of the bulk of the corresponding samples. The differences in reflection intensities between the simulated and the experimental patterns are due to the variation in the crystal orientation of the powder sample. To examine the thermal stabilities of complexes **1**−**3**, thermogravimetric analysis (TGA) experiments have been carried out. The TGA curve (Supporting Information, Figure S12) exhibits that a 11.4% weight loss is observed between 25 and 200 °C, which is consistent with four uncoordinated water molecules and one CH_3OH molecule departure (theoretical 11.1%, experimental 11.5%), indicating strong hydrogen-bonding interactions exist in **1**. The release of two coordinated water molecules (theoretical 4.0%, experimental 4.3%) for **2** and the release of two dissociative water molecules and one coordinated CH_3OH

dx.doi.org/10.1021/ic500183b | *Inorg. Chem.* 2014, 53, 5972−5985

molecule (theoretical 7.6%, experimental 7.5%) for **3** up to a high temperature (290 °C) may be ascribed to the strong coordination bond between Mn^{2+} ion and oxygen atoms and O−H···N strong hydrogen bonding. The coordination frameworks begin to decompose at 400 °C for **1**−**3**, and the long-range order disappears and comes into being an amorphous phase.

Anion-Exchange Properties of 1 and 2. Anion-induced crystal transformations, especially SC-SC transformations, have been widely investigated for coordination frameworks recently.[45,46] Herein, powder X-ray and well-defined single-crystal diffraction analysis methods were employed to monitor the related dynamic conversions between some crystalline solids. Note that for the related dynamic conversions between other MOFs, the product cannot be definitely characterized by the available methods, and they are, thus, not referred to herein. We investigated the anion-exchange reactions of these 2D and 3D architectures of **1** and **2**, respectively. After gently stirring the crystals of **1** (0.5 mmol) and **2** (0.5 mmol) in a 1:1 CH_3OH/H_2O solution containing $NaClO_4·H_2O$ (5 mmol) for 6 h, the crystals can retain their crystalline appearances. A remarkable SC-SC transformation was observed, and a 2D layer $\{[Cu(tatrz)_2(H_2O)_2](ClO_4)_2·4CH_3OH\}$ (**1a**) and a 2-fold interpenetrating 3D framework of $\{[Cu(tatrz)_2(H_2O)_2]\text{-}(ClO_4)_2·5.56H_2O\}_n$ (**2a**) were obtained.

For **1a**, each central Cu^{II} ion lies in the elongated octahedral coordination environment, which is somewhat similar to that of **1**. However, there is a slight difference on the fundamental structural units of **1** and **1a**. In **1a**, the central Cu^{II} ion lies in the inversion position, and two axial oxygen atoms are from two terminal coordinated aqua molecules, whereas, in **1**, two axial nitrogen atoms are from two NO_3^- anions. As shown in Figure 7a, each tatrz ligand in **1a** acts as a bridging bidentate ligand and links two neighboring Cu^{II} ions. Each Cu^{II} ion is coordinated with four neighboring Cu^{II} ions by four tatrz ligands to form a two-dimensional rhombohedral grid similar to that of **1**. The dihedral angles between atan rings and triazole moieties of tatrz are 73.4 and 87.8°, which is different from **1**. The 2D cation grid motif with the dimensionalities of 13.259(12) × 13.259(12) $Å^2$ are also densely stacked in an offset ABCABC··· stacking way (Figure 7b), and the free ClO_4^- anions are located between these neighboring 2D layers (Figure 8). This is quite different from that the nonporous structure of **1**; the result may be ascribed to different stacking ways between **1** and **1a** and different guest molecules or anions contained in the same 2D framework. Further, the coordinated aqua molecules (O5), the free ClO_4^- anions, and nitrogen atoms of triazole groups are also involved in O−H···O and O−H···N hydrogen bonds with relatively linear geometry (the bond angles of O−H···O and O−H···N in the range of 152 and 168°), which also extend the 2D framework of **1a** into the 3D hydrogen-bonding framework (Supporting Information, Figure S13), quite different from that of **1**. Such hydrogen-bonding roles are key and important for stablizing the 3D supramolecular framework.

X-ray single-crystal structural analysis indicated that both **2** and **2a** are isomorphous crystals. In **2a**, the central Cu^{II} ion lies in the inversion center and is six-coordinated by two aqua molecules and four $N_{triazole}$ atoms from four tatrz ligands. From the topological point, if the central Cu^{II} ion is considered as four connected nodes and the tatrz tecton is seen as two-connected linker, the overall framework of **2a** should be a 3D four-connected network with the Schläfli symbol of $6^5$8-$CdSO_4$ topology, the same as **2**. A 2-fold interpenetrating structure can be observed, and the pore size of 1D channel is 13.246(2) × 14.353(2) $Å^2$, in which free perchlorate anions are encapsulated as counteranions. It is also helpful to note that the coordinated aqua molecules (O1) and free ClO_4^- oxygen atoms (O5, O9) in **2a** are also involved in O−H···O (the bond angles of O−H··· O in the range of 160° and 176°). The weak forces play a crucial role in stabilizing the expanded 3D framework. In a word, the most obvious difference between **2** and **2a** is that BF_4^- anions in **2** were thoroughly replaced by ClO_4^- in **2a**. The other difference is that there are no guest solvent molecules in **2**, while 5.56 crystal lattice water molecules are trapped in the cavity of **2a** (Supporting Information, Figure S14).

Solvent-Exchange Properties during the Process of SC-SC Transformation. Generally, MOFs have low solubility and high stability in common solvents; therefore, these frameworks can retain their morphology through a solvent-assisted solid-state reaction, although in some examples the solid materials may lose their crystallinity. In recent years, previous researches also demonstrated that involved solvent molecules can induce SC-SC transformations. In most examples, guest moieties of diverse shapes and sizes can be encapsulated in the MOF cavities via various intermolecular interactions. Therefore, MOF products in such conversion process exhibit a certain shape flexibility and size specificity, and they have wide applications in many research fields such as selective molecular/ion recognition, separation, and molecular/ion sensors.[47] Although some related research in the construction of MOFs with framework structures by deliberately tuning different kinds of solvent molecules[48,49] or different component ratios of mixed solvents[50] have been reported, a particular series of MOF species that can be systematically tuned by the two factors in combination and also undergo structural transformations still remains largely unexplored thus far. To further investigate the effect of solvent-molecule exchanges on the SC-SC transformation, we employ **1a** as a precursor in DMF and thereby generate an isomorphic solvate of $\{[Cu(tatrz)_2(DMF)_2](ClO_4)_2·2H_2O\}_n$ (**1b**). X-ray analysis revealed that the 2D MOF families of **1a** and **1b** are supramolecular isomers even though they are topologically equivalent. The molecule moiety of **1a** is preserved in DMF, but it undergoes axial-ligand substitution upon dissolution. Significantly, when **1b** was immersed in CH_3OH/H_2O mixed solvents for 6 h, **1b** undergoes a solvent−ligand substitution reaction to yield **1a**, and the mutual solvent-induced conversions were successfully realized between **1a** and **1b**. These experimental results are of great significance in recognizing the anion and solvent effect upon coordination assemblies and their crystal transformations.

Inspired by the above-mentioned solvent-exchanges in the tatrz-Cu system, we exploited **1** as a precursor in methanol for 6 h to generate $\{[Cu(tatrz)_2(NO_3)_2]·0.6H_2O·4.4CH_3OH\}_n$ (**1c**). The structure of **1c** is essentially isostructural to **1**, with similar cell dimensions and the same gross structural features (detailed bond parameters can be obtained for the archived CIF file (CCDC-978550)). A careful investigation shows that the intercalated CH_3OH and aqua molecules play the key role in differentiating the two structures. Interestingly, when the same preparation method was employed with **1c** replacing **1** as a precursor, corresponding crystals, absolutely the same with **1**, were isolated, which was revealed by the X-ray analysis. A series of SC-SC transformations between the title complexes is shown in Scheme 1. The reversible transformation observed in these

dx.doi.org/10.1021/ic500183b | Inorg. Chem. 2014, 53, 5972−5985

Scheme 1. Synthesis of Complexes 1−3, 1a−3a, 1b, and 1c

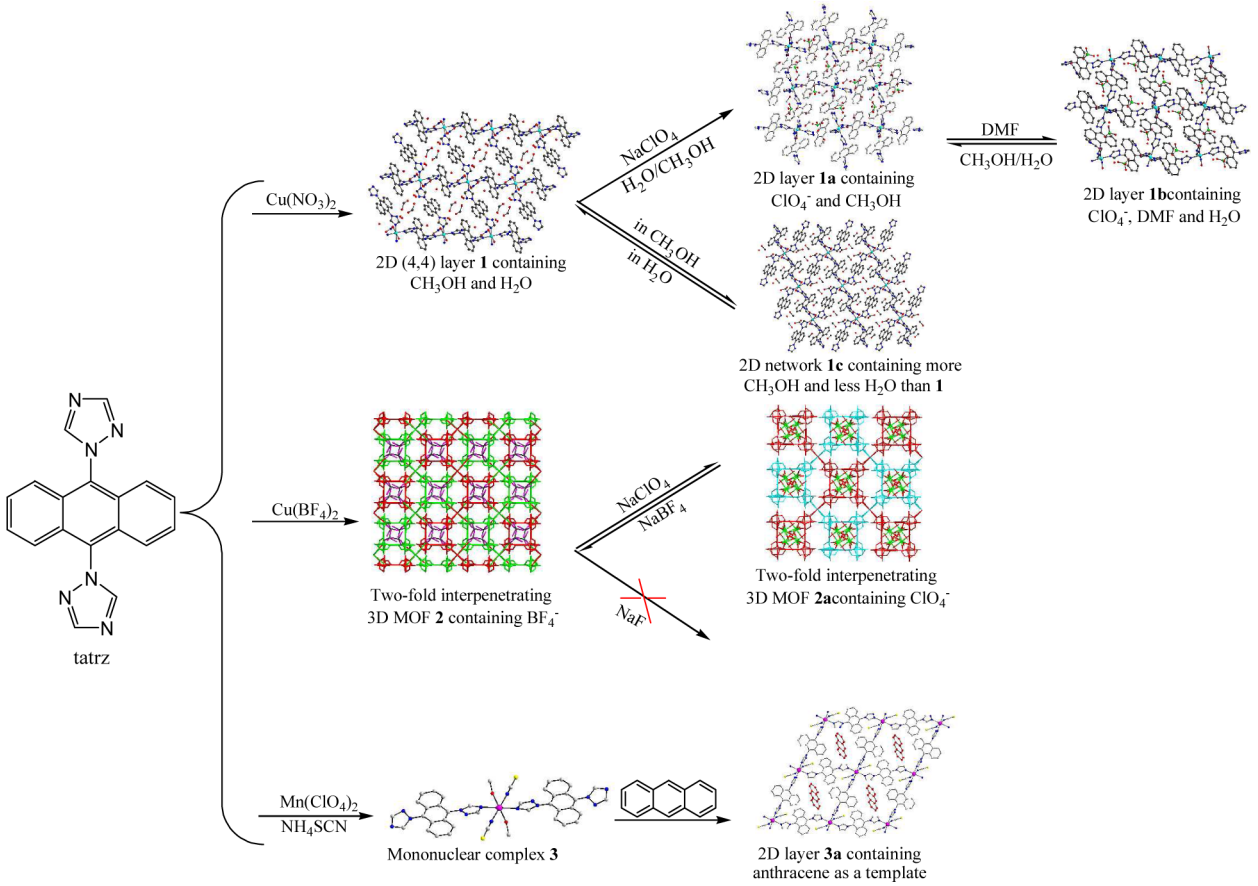

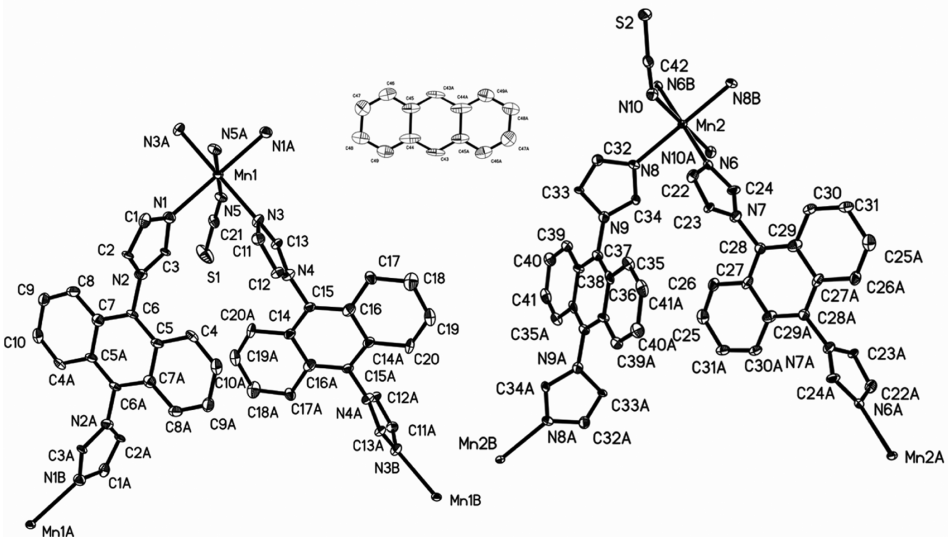

Figure 9. ORTEP diagram and atom labeling system for **3a**.

Cu(II) complexes could be due to two reasons: (i) local structural adjustment around a metal ion requires the variation of the coordination environment, and copper has versatile coordination modes; (ii) the Jahn−Teller effect of Cu(II) would facilitate the framework distortion.[51]

Organic Group Functionalized Aromatic Guest Loaded Host−Guest Complex. In addition to the anion-exchange and solvent-exchange reactions discussed above, confined spaces within self-assembled molecular containers can have a number of intriguing properties.[52] It is now obvious that the molecular behaviors within a confined space could be quite different from that in solution.[53] For instance, in the inner cavity of a self-assembled host, selective encapsulation can change and catalyze chemical reactions[54] or deliberately tune magnetic[55] and photoluminescent properties.[56] Inspired by the above-mentioned progress in the investigation of guest-exchange on 2D layer **1** and 3D framework **2**, we employ mononuclear complex **3** as a precursor to synthesize reactive

dx.doi.org/10.1021/ic500183b | Inorg. Chem. 2014, 53, 5972−5985

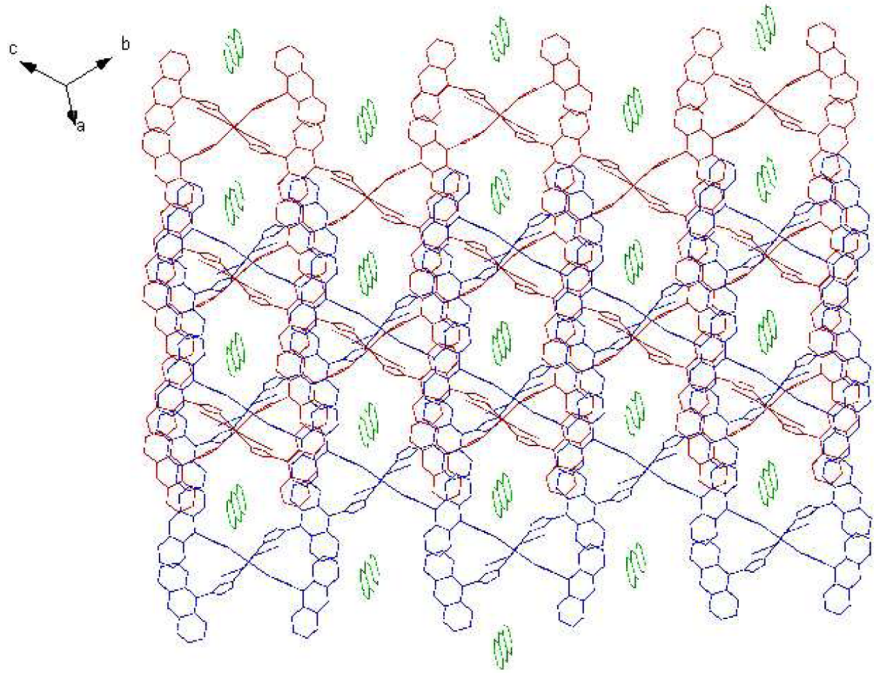

Figure 10. 2D framework of **3a** stacking in the ABAB··· way containing large 1D channels in which large aromatic molecules are located. Green, anthracene; blue and red, two neighboring 2D layers.

organic group functionalized aromatic guest loaded host−guest complex $\{[Mn(tatrz)_2(SCN)_2]\cdot(atan)\}_n$ (**3a**). After gently stirring **3** in trichloromethane containing atan for 6 h, through our careful observations, **3** was dissolved, and a remarkable reassembly process occurred. The mononuclear **3** was converted into the novel 2D coordination framework **3a**, encapsulating atan as an organic template, confirmed by X-ray diffraction structural analysis and ^{1}H NMR spectra (Supporting Information, Figure S15). Complex **3a** crystallizes in the triclinic crystal system, $P\bar{1}$ space group. The fundamental structural unit of **3a** includes two crystallographically unique six-coordinate Mn^{II} centers (Mn1 and Mn2), two bridging tatrz ligands, and two terminal-coordinated NCS^- anions (Figure 9). Each Mn^{II} center lies in an octahedral geometry and links four neighboring Mn^{II} centers through four bridging tatrz ligands, thus ultimately affording the 2D sheet structure with (4,4) topology along the *a* axis. The dihedral angle between atan rings and triazole moieties of tatrz of **3a** are 76° and 5.8°, respectively. The large 1D channels with the size of 14.027 × 14.027 Å^2 also can be observed. As is displayed in Figure 10, two adjacent planes (based on Mn1 and Mn2 centers, respectively) stack in the ABAB··· way. To the best of our knowledge, such large aromatic molecule atan as a template located in the 1D channel is the first reported in the metal−triazole coordination polymers.

Magnetic Properties. The magnetic data were collected in the temperature range of 2−300 K at an applied field of 1 kOe on a Quantum Design MPMS-5S SQUID magnetometer. The temperature dependence of the magnetic properties in the forms of χ_M and $\chi_M T$ for **2** and **2a** are shown in Supporting Information, Figure S16. Pascal's constants were applied to evaluate the diamagnetic correction. The $\chi_M T$ values are 0.395 and 0.40 cm^3 K mol^{-1}, respectively, for **2** and **2a** at room temperature, which can be expected spin-only values for an isolated Cu^{II} ion. With cooling, the $\chi_M T$ values for both **2** and **2a** almost keep a constant until 0.388 cm^3 K mol^{-1} at 18 K for **2** and 0.389 cm^3 K mol^{-1} at 5 K for **2a**, respectively. Further decreasing the temperature, the $\chi_M T$ values both decrease, reaching the minima of 0.38 and 0.44 cm^3 K mol^{-1} at 2 K for **2** and **2a**, respectively. This phenomenon indicates the paramagnetic properties of both complexes because the large ligand tatrz hardly mediates magnetic coupling between copper(II) ions. The linear fit via $\chi_M = C/(T - \theta)$ also confirms a Curie−Weiss behavior in the temperature range of 2−300 K with C = 0.396 and 0.407 cm^3 mol^{-1} K and θ = −0.32 and −0.71 cm^{-1} for **2** and **2a**, respectively, indicating very weak antiferromagnetic interactions between Cu^{II} ions in both of the two complexes.

Luminescent Properties. Aromatic organic molecules and inorganic−organic hybrid coordination complexes were investigated for their photoluminescent properties and for potential applications as luminescent materials, such as light-emitting diodes (LEDs).[57] Owing to the ability of adjusting the emission strength and wavelength of organic materials, the construction of inorganic−organic coordination complexes through the judicious incorporation of transition metal centers and conjugated organic spacers can be an efficient strategy for synthesizing new kinds of photoluminescent materials. As we know, a double bond is constituted by σ and π bonds, and the emissions of the organic ligands are usually ascribed to the $\pi^* \rightarrow n$ or $\pi \rightarrow \pi^*$ transitions.[58] It is then expected that the double bond-based ligand tatrz would exhibit photoluminescence property. Previous research also confirms that coordination polymers have the ability to affect the emission strength and wavelength of organic materials through the judicious incorporation of different central metal ions.[59−61] Cao's group has reported the photoluminescence properties of a series of Mn(II) complexes;[54c] therefore, it gives us an impetus to investigate the photoluminescent properties of complexes **3** and **3a**.

At ambient temperature, tatrz in DMSO is luminescent and exhibits a narrow emission maximum at 440 nm (λ_{ex} = 327

dx.doi.org/10.1021/ic500183b | Inorg. Chem. 2014, 53, 5972−5985

nm). Complex **3** exhibits a relatively weak blue fluorescent emission band at 439 nm upon excitation at 320 nm, while **3a** exhibits a relatively intense blue fluorescent emission band at 442 nm (λ_{ex} = 320 nm). As depicted in Figure 11, the main

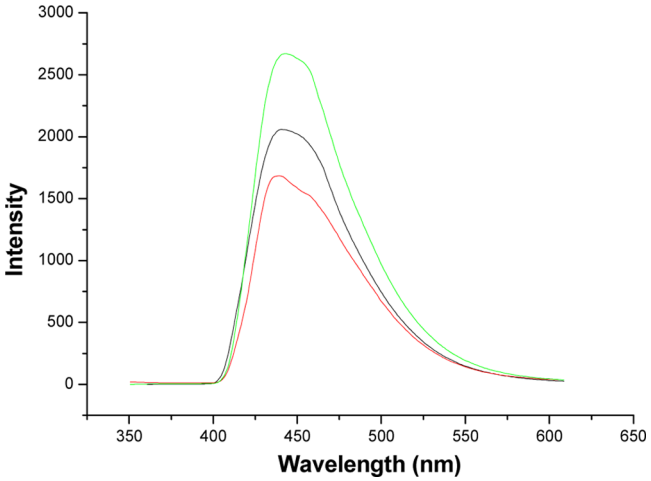

Figure 11. Emission spectra in DMSO solution at room temperature (1×10^{-4} mol/L for tatrz, **3**, and **3a**). All the compounds are excited at 320 and 327 nm. Black, tatrz; red, **3**; green, **3a**.

emission peaks of these coordination compounds are located at almost the same position (λ_{max} = 440 ± 2 nm) and exhibit a strong blue fluorescence with slightly different band shapes. All the coordination compounds also exhibit some low-energy emission peaks, which have positions and shapes similar to those of tatrz ligands. The emission peaks are neither metal-to-ligand charge transfer (MLCT) nor ligand-to-metal charge transfer (LMCT) in nature, and probably can be ascribed to the intraligand fluorescent emission since similar emission peaks can also be observed for the free tatrz ligand.[36h]

The emission spectra for tatrz, **3**, and **3a** in the solid state are displayed in Figure 12. The excited peaks of all the coordination compounds are located at 350 ± 5 nm. The main emission peaks are located at 552 nm for tatrz, 509 nm for **3**, and 530 nm for **3a**, respectively. They exhibit strong green

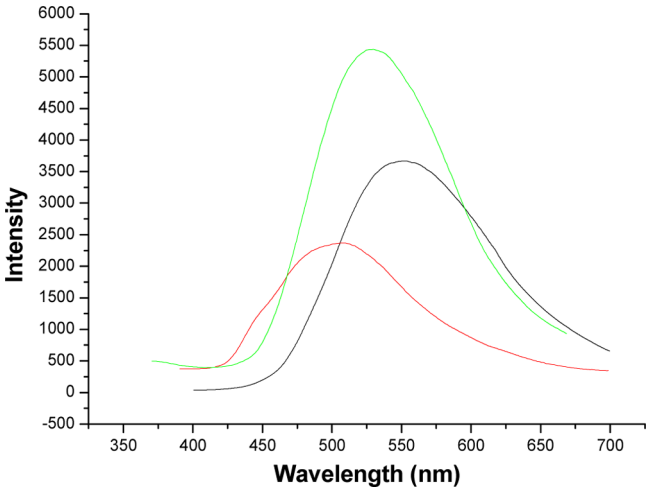

Figure 12. Emission spectra in the solid state at room temperature. All the compounds are excited at 380 ± 2 nm. Black, tatrz; red, **3**; green, **3a**.

fluorescence with slightly different band shapes. In comparison with that of the free tatrz ligand, complex **3a** in the solid state has a similar red shift. Combining previous studies, this red shift should be ascribed to LMCT transition, while the maximum wavelength and the intensity of excitation and emission in **3a** are red-shifted and stronger in comparison with those of **3**, which is likely due to a more extended π-conjugated system in **3a**.

Most importantly, the emission intensity of **3a** significantly increases upon adding 1−3 equiv of Mg^{2+} ions (from $MgCl_2$) with respect to **3a** (Figure 13). First, **3a** can be considered not to decompose in DMSO based on the control experiments. If **3a** decomposes in DMSO, then such luminescent enhancement with the increasing concentration of Mg^{2+} ions may mainly be ascribed to the interaction between $[Mn(tatrz)_2]^{2+}$ and Mg^{2+} ions. Therefore, a luminescence increase should also be observed for a similar system containing $[Mn(tatrz)_2]^{2+}$ moieties upon the addition of Mg^{2+} ions. The highest band at 441 nm is ca. twice as intense as the corresponding peak in DMSO solution without Mg^{2+} ions. To further understand this experimental phenomenon, the same experiments were made with the introduction of Ni^{2+} ions ($NiCl_2$) and Co^{2+} ions ($CoCl_2$) into the system. The results exhibit that the luminescence peaks do not enhance, but rather the luminescent intensities of **3a** are decreased. It is interesting that, upon adding Ca^{2+} ions ($CaCl_2$), the emission intensity of **3a** exhibits almost the same intensity as that seen for **3a**. The above experimental results support the idea that the luminescent emission of **3a** shows excellent selectivity for Mg^{2+} and that both complexes may be further considered as luminescent probes of Mg^{2+}.[62,63] To the best of our knowledge, this is the first report of multidimensional polymers based on triazole drivatives as luminescent probes of Mg^{2+}.

CONCLUSION

In conclusion, currently these porous molecular containers, also defined as capsules or flasks, have presented a number of attractive features. In this work the new multidentate ligand 1-(9-(1*H*-1,2,4-triazol-1-yl)anthracen-10-yl)-1*H*-1,2,4-triazole (tatrz) was designed and synthesized. With the help of such new tatrz building block, three novel coordination frameworks, namely, $\{[Cu(tatrz)_2(NO_3)_2]\cdot(CH_3OH)\cdot 4H_2O\}_n$ (**1**), $\{[Cu(tatrz)_2(H_2O)_2](BF_4)_2\}_n$ (**2**), and $[Mn(tatrz)_2(SCN)_2(CH_3OH)]\cdot 2H_2O$ (**3**) were isolated. For the 2D host framework of **1**, anion- and solvent-exchange experiments were investigated, indicating that guest NO_3^- anions and guest water molecules can be exchanged in an irreversible SC-SC transformation fashion, as evidenced by the exchanged crystalline product of $\{[Cu(tatrz)_2(H_2O)_2](ClO_4)_2\cdot 4CH_3OH\}$ (**1a**), $\{[Cu(tatrz)_2(DMF)_2](ClO_4)_2\cdot 2H_2O\}_n$ (**1b**), and $\{[Cu(tatrz)_2(NO_3)_2]\cdot 4.4CH_3OH\cdot 0.6H_2O\}_n$ (**1c**). Especially the solvent-exchange conversion is invertible between these crystalline frameworks (**1** and **1c**; **1a** and **1b**, as shown in Scheme 1), which also exhibits spongelike dynamic behavior with retention of crystalline integrity. Further, the 3D 2-fold interpenetrating framework **2** can also be transformed into another 2-fold interpenetrating 3D framework $\{[Cu(tatrz)_2(H_2O)_2](ClO_4)_2\cdot 5.56H_2O\}_n$ (**2a**) in a reversible SC-SC transformation fashion. However, when the light yellow crystals of mononuclear complex **3** were exposed to atan in trichloromethane, the crystals of **3** dissolved and reassembled into dark brown crystals of 2D crystalline coordination framework $\{[Mn(tatrz)_2(SCN)_2]\cdot(atan)\}_n$ (**3a**). Atan mole-

dx.doi.org/10.1021/ic500183b | Inorg. Chem. 2014, 53, 5972−5985

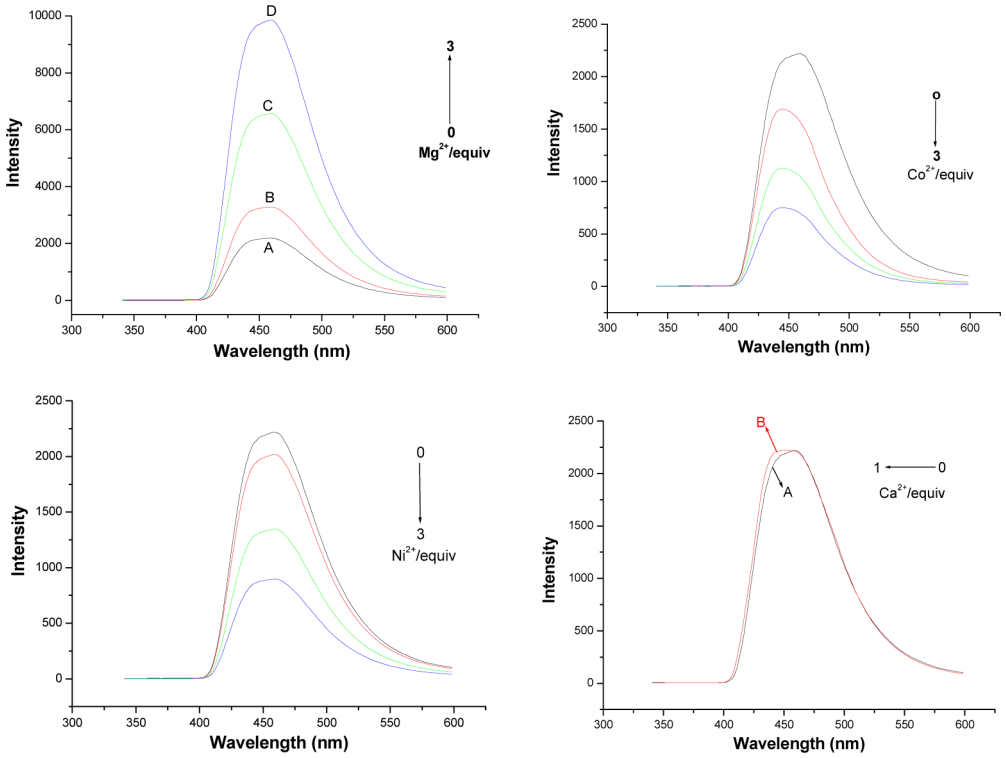

Figure 13. Emission spectra of complex **3a** in DMSO (10^{-3} M) at room temperature (excited at 315 nm) in the presence of 0–3 equiv of Mg^{2+} (top left), Co^{2+} (top right), Ni^{2+} (bottom left), and Ca^{2+} (bottom right). Line A, no addition; line B, 1 equiv; line C, 2 equiv; line D, 3 equiv.

cules were encapsulated as organic templates in the 2D grid of **3a**. Such a transformation process also represents the first example of metal–triazole coordination polymer containing atan and an exceedingly rare example of reassembly process from a 0D complex to a 2D sheet. Luminescent measurements indicate that **3a** is the first report of multidimensional polymers based on triazole drivatives as luminescent probes of Mg^{2+}. On the basis of this work, further synthesis and structural studies of the relationship between other porous functional coordination polymers with the newly designed tatrz building block in self-assembly are also underway in our lab.

■ ASSOCIATED CONTENT

Ⓢ Supporting Information

Listings of geometrical parameters of hydrogen bonds, ^{1}H NMR spectra, structure drawings, thermal dependence of the $\chi_M T$ curves, TGA plots, PXRD pattern for complexes **1**–**3**, **1a**–**3a**, **1b**, and **1c**. This material is free of charge via the Internet at http://pubs.acs.org. The crystallographic data for this Paper have been assigned to the following deposition CCDC numbers as CCDC-978547 (**1**), CCDC-978551 (**2**), CCDC-978553 (**3**), CCDC-978548 (**1a**) CCDC-978549 (**1b**), CCDC-978550 (**1c**), CCDC-978544 (**2a**), and CCDC-978545 (**3a**). These data can be obtained free of charge from The Cambridge Crystallographic Data Centre via www.ccdc.cam.ac.uk/data_request/cif.

■ AUTHOR INFORMATION

Corresponding Author

*E-mail: wangying790601@163.com. (Y.W.)

Notes

The authors declare no competing financial interest.

■ ACKNOWLEDGMENTS

This work was support financially by the Natural Science Foundation of Tianjin (Grant No. 11JCYBJC03600 and Grant No. 14JCQNJC05900), the Young Scientist Fund (Grant No. 21001080 and Grant No. 21301128), and the Program for Innovative Research Team in University of Tianjin (TD12-5038).

■ REFERENCES

(1) Kaskel, S. Porous Metal-Organic Frameworks. In *Handbook of Porous Solids;* Schuth, F., Sing, K. S. W., Weitkamp, J., Eds.; Wiley: Weinheim, Germany, **2002**; Vol. 2.
(2) MacGillivray, L. R. *Metal-Organic Frameworks;* Wiley-VCH: Hoboken, NJ, 2010.
(3) Férey, G. *Stud. Surf. Sci. Catal.* **2007**, *170A*, 66–86.
(4) Klein, N.; Senkovska, I.; Gedrich, K.; Stoeck, U.; Henschel, A.; Muller, U.; Kaskel, S. *Angew. Chem.* **2009**, *121*, 8667–8670; *Angew. Chem., Int. Ed.* **2009**, *48*, 9954–9957.
(5) Férey, G.; Mellot-Draznieks, C.; Serre, C.; Millange, F.; Dutour, J.; Surble, S.; Margiolaki, I. *Science* **2005**, *309*, 2040–2042.
(6) Koh, K.; Wong-Foy, A. G.; Matzger, A. J. *J. Am. Chem. Soc.* **2009**, *131*, 4184–4185.
(7) Koh, K.; Wong-Foy, A. G.; Matzger, A. J. *Angew. Chem.* **2008**, *120*, 689–692; *Angew. Chem., Int. Ed.* **2008**, *47*, 677–680.
(8) Rowsell, J. L. C.; Millward, A. R. K.; Park, S.; Yaghi, O. M. *J. Am. Chem. Soc.* **2004**, *126*, 5666–5667.
(9) Collins, D. J.; Zhou, H.-C. *J. Mater. Chem.* **2007**, *17*, 3154–3160.
(10) Panella, B.; Hirscher, M.; Pütter, H.; Müller, U. *Adv. Funct. Mater.* **2006**, *16*, 520–524.
(11) Mulfort, K. L.; Farha, O. K.; Malliakas, C. D.; Kanatzidis, M. G.; Hupp, J. T. *Chem.—Eur. J.* **2010**, *16*, 276–281.
(12) (a) Küsgens, P.; Rose, M.; Senkovska, I.; Fröde, H.; Henschel, A.; Siegle, S.; Kaskel, S. *Microporous Mesoporous Mater.* **2009**, *120*, 325–330. (b) Biswas, S.; Grzywa, M.; Nayek, H. P.; Dehnen, S.; Senkovska, I.; Kaskel, S.; Volkmer, D. *Dalton Trans.* **2009**, 6487–6495.

(13) Dybtsev, D. N.; Chun, H. S.; Yoon, H.; Kim, D.; Kim, K. *J. Am. Chem. Soc.* **2004**, *126*, 32−33.
(14) Car, A.; Stropnik, C.; Peinemann, K.-V. *Desalination* **2006**, *200*, 424−426.
(15) Ma, S.; Sun, D.; Wang, X.-S.; Zhou, H.-C. *Angew. Chem.* **2007**, *119*, 2510−2514; *Angew. Chem., Int. Ed.* **2007**, *46*, 2458−2462.
(16) Czaja, A. U.; Trukhan, N.; Müller, U. *Chem. Soc. Rev.* **2009**, *38*, 1284−1293.
(17) Ma, L.; Abney, C.; Lin, W. *Chem. Soc. Rev.* **2009**, *38*, 1248−1256.
(18) Lee, J. Y.; Farha, O. K.; Roberts, J.; Scheidt, K. A.; Nguyen, S. B.; Hupp, T. J. T. *Chem. Soc. Rev.* **2009**, *38*, 1450−1459.
(19) Horcajada, P.; Serre, C.; Vallet-Regi, M.; Sebban, M.; Taulelle, F.; Férey, G. *Angew. Chem.* **2006**, *118*, 6120−6124; *Angew. Chem., Int. Ed.* **2006**, *45*, 5974−5978.
(20) An, J.; Geib, S. J.; Rosi, N. L. *J. Am. Chem. Soc.* **2009**, *131*, 8376−8377.
(21) Fletcher, A. J.; Thomas, K. M.; Rosseinsky, M. J. *J. Solid State Chem.* **2005**, *178*, 2491−2510.
(22) (a) Kreno, L. E.; Leong, K. O.; Farha, K.; Allendorf, M.; Duyne, R. P.; Hupp, V. J. T. *Chem. Rev.* **2012**, *112*, 1105−1125. (b) Lu, G.; Hupp, J. T. *J. Am. Chem. Soc.* **2010**, *132*, 7832−7833.
(23) Horike, S.; Shimomura, S.; Kitagawa, S. *Nat. Chem.* **2009**, *1*, 695−704.
(24) (a) Kawano, M.; Fujita, M. *Coord. Chem. Rev.* **2007**, 2592−2605. (b) Kitagawa, S.; Matsuda, R. *Coord. Chem. Rev.* **2007**, *251*, 2490−2509.
(25) (a) Maji, T. K.; Kitagawa, R. S. *Nat. Mater.* **2007**, *6*, 142−148. (b) Park, H. J.; Lim, D.-W; Yang, W. S.; Oh, T.-R; Suh, M. P. *Chem.—Eur. J.* **2011**, *17*, 7251−7260.
(26) Yin, Z.; Zeng, M.-H. *Sci. China: Chem.* **2011**, *54*, 1371−1394.
(27) (a) Kitagawa, S.; Uemura, K. *Chem. Soc. Rev.* **2005**, *34*, 109−119. (b) Hoang, T.; Lauher, J. W.; Fowler, F. W. *J. Am. Chem. Soc.* **2002**, *124*, 10656−10657. (c) Hu, C. H.; Englert, U. *Angew. Chem.* **2005**, *117*, 2321−2323; *Angew. Chem., Int. Ed.* **2005**, *44*, 2281−2283. (d) Hanson, K.; Calin, N.; Bugaris, D.; Scancella, M.; Sevov, S. C. *J. Am. Chem. Soc.* **2004**, *126*, 10502−10503. (e) Zhang, Y. J.; Liu, T.; Kanegawa, S.; Sato, O. *J. Am. Chem. Soc.* **2009**, *131*, 7942−7943.
(28) (a) Wu, C. D.; Lin, W. B. *Angew. Chem.* **2005**, *117*, 1991−1997; *Angew. Chem., Int. Ed.* **2005**, *44*, 1958−1961. (b) Lee, E. Y.; Suh, M. P. *Angew. Chem.* **2004**, *116*, 2858−2861; *Angew. Chem., Int. Ed.* **2004**, *43*, 2798−2801. (c) Sun, J.; Dai, F.; Yuan, W.; Bi, W.; Zhao, X.; Sun, W.; Sun, D. *Angew. Chem.* **2011**, *123*, 7199−7202; *Angew. Chem., Int. Ed.* **2011**, *50*, 7061−7064. (d) Eddaoudi, M.; Kim, J.; Rosi, N.; Vodak, D.; Wachter, J.; O'Keeffe, M.; Yaghi, O. M. *Science* **2002**, *295*, 469−472.
(29) (a) Iordanidis, L.; Kanatzidis, M. G. *Angew. Chem.* **2000**, *112*, 2003−2006; *Angew. Chem., Int. Ed.* **2000**, *39*, 1927−1930. (b) Ranford, J. D.; Vittal, J. J.; Wu, D. Q. *Angew. Chem.* **1998**, *110*, 1159−1162; *Angew. Chem., Int. Ed.* **1998**, *37*, 1114−1116. (c) Toh, N. L.; Nagarathinam, M.; Vittal, J. J. *Angew. Chem.* **2005**, *117*, 2205−2209; *Angew. Chem., Int. Ed.* **2005**, *44*, 2237−2241. (d) Cohen, S. M. *Chem. Sci.* **2010**, *1*, 32−36.
(30) Wang, Y.; Cheng, P.; Song, Y.; Liao, D.-Z.; Yan, S.-P. *Eur. Chem. J.* **2007**, *13*, 8133−8138.
(31) (a) Custelcean, R. *Curr. Opin. Solid State Mater. Sci.* **2009**, *13*, 68−75. (b) Custelcean, R.; B. Moyer, A. *Eur. J. Inorg. Chem.* **2007**, 1321−1340.
(32) Recent reviews on anion receptors: (a) Wenzel, M.; Hiscock, J. R.; Gale, P. A. *Chem. Soc. Rev.* **2012**, *41*, 480−520. (b) Gale, P. A. *Chem. Commun.* **2011**, *47*, 82−86. (c) Gale, P. A. *Chem. Soc. Rev.* **2010**, *39*, 3746−3771.
(33) (a) Mercer, D. J.; Loeb, S. J. *Chem. Soc. Rev.* **2010**, *39*, 3612−3620. (b) Amendola, V.; Fabbrizzi, L. *Chem. Commun.* **2009**, 513−531. (c) Steed, J. W. *Chem. Soc. Rev.* **2009**, *38*, 506−519.
(34) Kubik, S. *Chem. Soc. Rev.* **2010**, *39*, 3648−3663.
(35) (a) Klingele, M. H.; Brooker, S. *Coord. Chem. Rev.* **2003**, *241*, 119−132. (b) Ferrer, S.; Haasnoot, J. G.; Reedijk, J.; Müller, E.; Cingi, M. B. M. A.; Lanfranchi, M.; Lanfredi, M.; Ribas, J. *Inorg. Chem.* **2000**, *39*, 1859−1867. (c) Yi, L.; Ding, B.; Zhao, B.; Cheng, P.; Liao, D. Z.; Yan, S. P.; Jiang, Z. H. *Inorg. Chem.* **2004**, *43*, 33−43. (d) Zhang, J. P.; Chen, X. M. *Chem. Commun.* **2006**, 1689−1699. (e) Zhai, Q. G.; Wu, X. Y.; Chen, S. M.; Lu, C. Z.; Yang, W. B. *Cryst. Growth Des.* **2006**, *6*, 2126−2135.
(36) (a) Tang, L.-F.; Wang, Z.-H.; Chai, J.-F.; Leng, X.-B.; Wang, J.-T.; Wang, H.-G. *J. Organomet. Chem.* **2002**, *642*, 179−185. (b) Long, Y.; Yang, X.; Lu, T.; Cheng, P. *Cryst. Growth Des.* **2005**, *5*, 1215−1219. (c) Albada, G. A.; Guijt, R. C.; Haasnoot, J. G.; Lutz, M. A.; Spek, L.; Reedijk, J. *Eur. J. Inorg. Chem.* **2000**, 121−126. (d) Ke, X.-J.; Li, D.-S.; Zhao, J.; Bai, L.; Yang, J.-J.; Duan, Y.-P. *Inorg. Chem. Commun.* **2012**, *21*, 129−132. (e) Chen, C.; Ma, J.-F.; Liu, B.; Yang, J.; Liu, Y.-Y. *Cryst. Growth Des.* **2011**, *11*, 4491−4497. (f) Wang, Y.; Cheng, P.; Song, Y.; Liao, D.-Z.; Yan, S.-P. *Chem.—Eur. J.* **2007**, *13*, 8131−8138. (g) Wang, Y.; Long, Y.; Yang, X.; Ding, B.; Cheng, P.; Liao, D.-Z.; Yan, S.-P. *Inorg. Chem.* **2006**, *45*, 5822−5829. (h) Ding, B.; Yi, L.; Wang, Y.; Cheng, P.; Liao, D.-Z.; Yan, S.-P.; Jiang, Z.-H.; Song, H.-B.; Wang, H.-G. *Dalton Trans.* **2006**, 665−675. (i) Wang, Y.; Ding, B.; Cheng, P.; Liao, D.-Z.; Yan, S.-P. *Inorg. Chem.* **2007**, *46*, 2002−2010.
(37) (a) Yang, W. J.; Kim, C. H. M.; Jeong, Y.; Lee, S. K.; Piao, M. J.; Jeon, S. J.; Cho, B. R. *Chem. Mater.* **2004**, *16*, 2783−2789. (b) Ishikawa, J.; Sakamoto, H.; Nakao, S.; Wada, H. *J. Org. Chem.* **1999**, *64*, 1913−1921. (c) Vollmer, M. S.; Wöthner, F.; Effenberger, F.; Emele, P.; Meyer, D. U.; Stümpfig, T.; Port, H.; Wolf, H. C. *Chem.—Eur. J.* **1998**, *4*, 260−269. (d) Ihmels, H.; Meiswinkel, A.; Mohrschladt, C. *Org. Lett.* **2000**, *2*, 2865−2867.
(38) (a) Zweig, A.; Maurer, A. H.; Roberts, B. G. *J. Org. Chem.* **1967**, *32*, 1322−1329. (b) Mauldingand, D. R.; Roberts, B. G. *J. Org. Chem.* **1969**, *34*, 1734−1736. (c) Giménez, R.; Piñol, M.; Serrano, J. L. *Chem. Mater.* **2004**, *16*, 1377−1383.
(39) Jones, S.; Atherton, J. C. C. *Synth. Commun.* **2001**, *31*, 1799−1802.
(40) *SHELXS 97,* Program for the Solution of Crystal Structures; Sheldrick, G.M., Ed.; University of Götingen: Götingen, Germany, 1997.
(41) *SHELXL 97,* Program for the Refinement of Crystal Structures; Sheldrick, G.M., Ed.; University of Götingen: Götingen, Germany, 1997.
(42) Ferrer, S.; Lloret, F.; Bertomeu, I.; Alzuet, G.; Borrás, J.; García-Granda, S.; Liu-González, M.; Haasnoot, J. G. *Inorg. Chem.* **2002**, *41*, 5821−5830.
(43) *PLATON,* A Multipurpose Crystallographic Tool; Spek, A. L., Ed.; Utrecht University: Utrecht, The Netherlands, 2001.
(44) (a) Myshakina, N. S.; Ahmed, Z.; Asher, S. A. *J. Phys. Chem. B* **2008**, *112* (38), 11873−11877. (b) Zhao, G.-J.; Han, K.-L. *Acc. Chem. Res.* **2012**, *45* (3), 404−413. (c) Tainter, C. J.; Ni, Y.; Shi, L.; Skinner, J. L. *J. Phys. Chem. Lett.* **2013**, *4* (1), 12−17.
(45) Fu, J.; Li, H.; Mu, Y.; Hou, H.; Fan, Y. *Chem. Commun.* **2011**, *47*, 5271−5273.
(46) Halper, S. R.; Do, L.; Stork, J. R.; Cohen, S. M. *J. Am. Chem. Soc.* **2006**, *128*, 15255−15268.
(47) (a) Chu, Q.; Swenson, D. C.; MacGillivrary, L. R. *Angew. Chem.* **2005**, *117*, 3635−3638; *Angew. Chem., Int. Ed.* **2005**, *44*, 3569−3572. (b) Blake, A. J.; Champness, N. R.; Chung, S. S. M.; Li, W.-S.; Schröder, M. *Chem. Commun.* **1997**, 1675−1676. (c) Xue, X.; Wang, X.-S.; Xiong, R.-G.; You, X. Z.; Abrahams, B. F.; Che, C.-M.; Ju, H.-X. *Angew. Chem.* **2002**, *114*, 3068−3070; *Angew. Chem., Int. Ed.* **2002**, *41*, 2944−2946.
(48) (a) Deiters, E.; Bulach, V.; Hosseini, M. W. *Chem. Commun.* **2005**, 3906−3908. (b) Dobrzańska, L.; Lloyd, G. O.; Esterhuysen, C.; Barbour, L. J. *Angew. Chem.* **2006**, *118*, 5988−5991; *Angew. Chem., Int. Ed.* **2006**, *45*, 5856−5859. (c) Kitagawa, S.; Noro, S.; Nakamura, T. *Chem. Commun.* **2006**, 701−707. (d) Chesman, A. S. R.; Turner, D. R.; Deacon, G. B.; Batten, S. R. *Chem. Commun.* **2010**, *46*, 4899−4901.
(49) (a) Warren, M. R.; Brayshaw, S. K.; Johnson, A. L.; Schiffers, S.; Raithby, P. R.; Easun, T. L.; George, M. W.; Warren, J. E.; Teat, S. J. *Angew. Chem.* **2009**, *121*, 5821−5824; *Angew. Chem., Int. Ed.* **2009**, *48*, 5711−5714. (b) Cheng, X.-N.; Zhang, W.-X.; Chen, X.-M. *J. Am. Chem. Soc.* **2007**, *129*, 15738−15739. (c) Neville, S. M.; Halder, G. J.; Chapman, K. W.; Duriska, M. B.; Southon, P. D.; Cashion, J. D.;

Létard, J. F.; Moubaraki, B. K.; Murray, S.; Kepert, C. J. *J. Am. Chem. Soc.* **2008**, *130*, 2869−2876.
(50) (a) Seidel, S. R.; Stang, P. J. *Acc. Chem. Res.* **2002**, *35*, 972−983. (b) Boyer, J. L.; Kuhlman, M. L.; Rauchfuss, T. B. *Acc. Chem. Res.* **2007**, *40*, 233−242. (c) Therrien, B.; Süss-Fink, G.; Govindaswamy, P.; Renfrew, A. K.; Dyson, P. J. *Angew. Chem.* **2008**, *120*, 3833−3836; *Angew. Chem., Int. Ed.* **2008**, *47*, 3773−3776.
(51) Kasai, K.; Fujita, M. *Chem.—Eur. J.* **2007**, *13*, 3089−3105.
(52) Li, C.-P.; Du, M. *Chem. Commun.* **2011**, *47*, 5958−5972.
(53) Braga, D.; Maini, L.; Mazzeo, P. P.; Ventura, B. *Chem.—Eur. J.* **2010**, *16*, 1553−1559.
(54) Liu, Q.-K.; Ma, J.-P.; Dong, Y.-B. *J. Am. Chem. Soc.* **2010**, *132*, 7005−7017.
(55) Rebek, J. *Acc. Chem. Res.* **2009**, *42*, 1660−1668.
(56) (a) Wang, Z.; Chen, G.; Ding, K. *Chem. Rev.* **2009**, *109*, 322−359. (b) Pluth, M. D. R.; Bergman, G.; Raymond, K. N. *Science* **2007**, *316*, 85−88. (c) Yoshizawa, M.; Tamura, M.; Fujita, M. *Science* **2006**, *312*, 251−254. (d) Kang, J. M.; Hilmersson, G.; Santamaria, J.; Rebek, J. *J. Am. Chem. Soc.* **1998**, *120*, 3650−3656. (e) Hasting, C. J.; Fiedler, D.; Bergman, R. G.; Raymond, K. N. *J. Am. Chem. Soc.* **2008**, *130*, 10977−10983. (f) Yoshizawa, M.; Takeyama, Y.; Okano, T.; Fujita, M. *J. Am. Chem. Soc.* **2003**, *125*, 3243−3247.
(57) (a) Halder, G. J.; Kepert, C. J.; Moubaraki, B.; Murray, K. S.; Cashion, J. D. *Science* **2002**, *298*, 1762−1765. (b) Ono, K.; Yoshizawa, M.; Akita, M.; Kato, T.; Tsunobuchi, Y.; Ohkoshi, S.-I.; Fujita, M. *J. Am. Chem. Soc.* **2009**, *131*, 2782−2783. (c) Southon, P. D.; Liu, L.; Fellows, E. A.; Price, D. J.; Halder, G. J.; Chapman, K. W.; Moubaraki, B. K.; Murray, S.; Létard, J.-F.; Kepert, C. J. *J. Am. Chem. Soc.* **2009**, *131*, 10998−11009.
(58) (a) Dalgarno, S. J.; Tucker, S. A.; Bassil, D. B.; Atwood, J. L. *Science* **2005**, *309*, 2037−2039. (b) Dong, Y.-B.; Wang, P.; Ma, J.-P.; Zhao, X.-X.; Wang, H.-Y.; Tang, B.; Huang, R.-Q. *J. Am. Chem. Soc.* **2007**, *129*, 4872−4873. (c) McManus, G. J.; Perry, J. J.; Perry, M.; Wagner, B. D.; Zaworotko, M. J. *J. Am. Chem. Soc.* **2007**, *129*, 9094−9101. (d) Wang, P.; Ma, J.-P.; Dong, Y.-B.; Huang, R.-Q. *J. Am. Chem. Soc.* **2007**, *129*, 10620−10621. (e) Wang, P.; Ma, J.-P.; Dong, Y.-B. *Chem.—Eur. J.* **2009**, *15*, 10432−10445. (f) Jiang, Y.-Y.; Ren, S.-K.; Ma, J.-P.; Liu, Q.-K.; Dong, Y.-B. *Chem.—Eur. J.* **2009**, *15*, 10742−10746.
(59) Maspoch, D.; Domingo, N.; Roques, N.; Wurst, K.; Tejada, J.; Rovira, C.; Ruiz-Molina, D.; Veciana, J. *Chem.—Eur. J.* **2007**, *13*, 8153−8163.
(60) Bunz, U. H. F. *Chem. Rev.* **2000**, *100*, 1605−1644.
(61) Tzeng, B. C.; Chiu, T. H.; Chen, B. S.; Lee, G. H. *Chem.—Eur. J.* **2008**, *14*, 5237−5245.
(62) (a) Sun, D.; Xu, H. R.; Yang, C. F.; Wei, Z. H.; Zhang, N.; Huang, R. B.; Zheng, L. S. *Cryst. Growth Des.* **2010**, *10*, 4642−4649. (b) Sun, D.; Zhang, N.; Huang, R. B.; Zheng, L. S. *Cryst. Growth Des.* **2010**, *10*, 3699−3709. (c) Gong, Y.; Li, J. H.; Wu, T.; Qin, J. B.; Cao, R.; Li, J. *CrystEngComm* **2012**, *14*, 663−669.
(63) Zhao, B.; Gao, H.-L.; Chen, X.-Y.; Cheng, P.; Shi, W.; Liao, D.-Z.; Yan, S.-P.; Jiang, Z.-H. *Chem.—Eur. J.* **2006**, *12*, 149−158.

dx.doi.org/10.1021/ic500183b | *Inorg. Chem.* 2014, 53, 5972−5985